

Hybrid Convolutional Neural Network Method for Robust Brain Stroke Diagnosis and Segmentation

Sercan Yalcin

Abstract— Artificial intelligence with deep learning methods has been employed by a majority of researchers in medical image classification and segmentation applications for many years. In this study, a hybrid convolutional neural network (CNN) model has been proposed for diagnosing brain stroke from the dataset consisting of computed tomography (CT) brain images. The model inspired by C-Net consists of multiple concatenation layers of the networks, and prevents the concatenation of convolutional feature maps to evince the mapping process. The structures of the convolutional index and residual shortcuts of the INet model are also integrated into the proposed CNN model. In the output layer of the model, it is split into two classes as whether there is a stroke or not in a brain image, and then the region of the stroke in the image is segmented. Tremendous analyzes have been conducted in terms of many benchmarks using Python programming. The proposed method shows better performance than some other current CNN-based methods by 99.54% accuracy and 99.1% Matthews correlation coefficient (MCC) in the diagnosis of brain stroke. The proposed method can alleviate the work of most medical staffs and facilitate the process of the patient's remedy.


Index Terms— Artificial intelligence, brain stroke diagnosis, convolutional neural networks, deep learning.

I. INTRODUCTION

IT IS HOPED that humanity will use artificial intelligence-based medical technologies to create applications that help society by fusing social responsibility consciousness with technological understanding [1].

Brain stroke is one of the deadliest diseases in the world and rapid diagnosis is very important in the medical treatment process. [2]. Patients who exhibit certain symptoms may have had an ischemic or hemorrhagic stroke. When blood clots prevent or drastically restrict blood flow to the brain, an ischemic stroke results. After an ischemic stroke, patients may also develop stroke bleeding, which is a dangerous consequence.

SERCAN YALÇIN, is with Department of Computer Engineering University of Adiyaman University, Adiyaman, Turkey (e-mail: svancin@adiyaman.edu.tr).

 <https://orcid.org/0000-0003-1420-2490>

Manuscript received June 11, 2022; accepted Aug 17, 2022.
DOI: [10.17694/bajece.1129233](https://doi.org/10.17694/bajece.1129233)

While hemorrhage happens as a result of a stroke, blood traveling to other surrounding brain tissues, blood vessels bursting due to their rigidity, or both. A concussion, high blood pressure, bleeding problems, aneurysms, and arteriovenous malformation are the main causes of hemorrhagic brain stroke [3]. The care and outlook for stroke patients must be improved because it is well known that strokes are a severe health issue. Therefore, quick and accurate diagnostic techniques are required. The terms "brain imaging techniques" relate to magnetic resonance imaging (MRI) and computed tomography (CT). They give the doctors the patient consults a hint as to how to keep the patient under initial control. Additionally, there are a number of imaging methods for examining the brain, such as magnetoencephalography, functional magnetic resonance imaging, emission positron tomography, and X-ray and optical imaging. The most widely used imaging technique is the CT scan. This is mostly because patients may receive its images, which are less expensive than those from other imaging systems. The first step in providing patients with an appropriate diagnosis and course of treatment is the ability to predict brain stroke using CT imaging [4].

Convolutional neural networks (CNNs), which are deep learning techniques based on artificial intelligence, have made significant progress in the recognition of biomedical images. When working with medical images, CNNs are employed for semantic segmentation procedures where each pixel in the image is labeled by a neighboring object or region. Along with classification, picture segmentation is a crucial job that is used to increase the accuracy of diagnoses. The primary goal and task of the medical image, which goes through a pixel-level categorization procedure, is actually image segmentation [5]. A deep CNN-based method for the identification and classification of acute ischemic stroke was presented by Lo et al. [6] utilizing CT images. The imaging dataset for the is made up of 573 CT scans from 96 patients who had ischemic strokes and 96 healthy controls (681 images). Radiologists were able to diagnose acute ischemic stroke thanks to transfer learning, which was successful in establishing a specific scratch training approach for a specific scanner. On MRI pictures of patients, Tomitaa et al. [7] suggested a deep neural network approach for segmenting severely wounded brain lesions. A total of 239 pictures from a dataset of patients with persistent ischemic stroke were processed using the suggested scheme. A new

zooming technique was used in performance analyses of 3D segmentation models with residual networks. Deep learning and CNN were suggested by Gaidhani et al. [5] as a technique for identifying brain stroke using an MRI. Brain stroke MRI pictures might be separated into normal and abnormal images using the suggested strategy. Semantic segmentation was also used to identify anomalous regions. LeNet and SegNet are two different CNN types that are utilized by the suggested methodology [8]. LeNet is a CNN deep architecture built on encoder-decoder technology. SegNet is a sophisticated and complete CNN model for semantic pixel-wise segmentation. For the purpose of segmenting images, the encoder-decoder CNN architecture known as UNet [9] was created. This architecture's major objective is to provide a shared negotiation network with successive layers that uses upsampling operators in place of pooling operators. In order to dynamically separate acute ischemic stroke lesions from multi-directional MRIs, Liu et al. [10] presented a new deep residual CNN. Any enhancements made by INet [12] are guaranteed when the original U-Net contains residual shortcuts known as ResUNet [11]. The degradation issue was improved by the Res-CNN using additional data from MRIs [12]. The definition of ResDenseUNet [13], a different model to compare with the suggested model with dense linkages known as DenseINet [12], is when residual shortcuts are added to the original DenseUNet [12]. Data augmentation and data aggregation techniques were employed to enhance the amount of training images prior to training the network model. On two acute ischemic stroke datasets, seven neural networks were trained, and the outcomes were thoroughly examined. CNN combined with random forests was used by Saragih et al. [14] to conduct ischemic stroke detection based on a patient's CT scan. In this approach, in the categorization of data based on feature extraction with CNN, the fully linked layer has been replaced by completely random forests. 10% of the data set was test data when the suggested procedure was applied. A new CNN design dubbed C-Net that combines various networks was proposed by Barzekar and Yu [15]. On the BreakHis and Osteosarcoma datasets, the C-Net was used for the categorization of histological picture. For both datasets, the C-Net model was effective, yielding no misclassifications. For the purpose of identifying movement-related brain MR artifacts, Oksuz [16] proposed dense CNNs and a residual U-Net architecture. A method based on MR physics was used to create artificial artifacts. A residual U-net network tuned using corrupted data helped to improve the observed artifacts. The architecture, which handles artifact detection and correction, produced higher-quality images and made it possible to segment brain strokes more precisely. A novel technique for cerebral vascular segmentation without the requirement for physical intervention was put out by Deshpande et al. [17]. In order to disclose vascular geometric aspects and categorize vascular anatomy, the scientists also provided a model by skeletonizing the binary segment map. They divided MR and CT angiograms using an active contour-based method. This method combines probabilistic grain-enhancing filtering with a Hessian framework. Additionally, the vessel centerlines and diameters have been calculated using this method in order to determine the geometrical characteristics of the vasculature. Dimension-

fusion-UNet (D-UNet), a brain segmentation model suggested by Zhou et al. [18], mixes 2D and 3D convolution during the encoding phase. In comparison to 2D networks, the suggested model performs better in segmentation. Compared to 3D networks, the model requires substantially less computational effort. To lessen the data imbalance between positive and negative instances for the network's training, the scientists also developed a new loss function called Enhance Mixing Loss (EML).

The brain CT pictures have been examined in this paper to assess whether or not a stroke has occurred. Additionally, the section of the brain that the radiologist examined has been calculated after the brain strokes in the photographs were segmented. A deep learning algorithm based on CNN has been suggested. In the brain CT images of the dataset collected from the Ministry of Health of the Republic of Turkey, the suggested model recognizes and categorizes brain strokes. By using the segmentation method, the model can identify and forecast the stroke region. Other current CNN models, including ResNet50v2 [19], UNet [9], DeepLabV3 [20], ResUNet [11], DenseINet [12], ResDenseUNet [13], and C-Net [15], have also been used to examine performance for classifying and segmenting brain strokes in the same CT brain images. A variety of evaluations have been performed based on comparisons between the performance results that were produced.

The following are the paper's main contributions:

- To classify and segment the brain pictures, a deep hybrid model based on C-Net and INet is provided. The proposed model might be crucial for the quick identification and treatment of brain stroke.
- Preprocessing techniques have been used to improve the contrast of the image, making it easier to identify the stroke-affected area from the brain scans. Additionally, the proposed model successfully designs the layers of convolution, pooling, dropout, and fully connected, and it takes convolutional index and residual shortcuts into account.
- The Ministry of Health of the Republic of Turkey provided the study with an actual data set. The collection contains CT images in the Digital Imaging and Communications in Medicine (DICOM) format that are not stroke-related, ischemic, hemorrhagic, or overlay.
- According on experimental performance findings, the suggested model outperforms DenseINet, ResDenseUNet, and C-Net.
- Although this study has been inspired by our previous study [21] and the data set used was the same, it can be said that it is original in terms of the proposed method and an innovative approach is presented.

The rest of the paper organization is as follows: Section 2 explains the material and method. Experimental analyzes and results are presented in Section 3. Both classification and segmentation results are evaluated, and then compared to other recent studies. Finally, in Section 4, the study is concluded.

II. MATERIAL AND METHOD

In this study, a new hybrid deep learning scheme is proposed for brain stroke diagnosis by taking advantage of C-Net and INet CNN architectures. INet is a CNN architecture that can increase receptive areas by incrementally increasing the kernel sizes of convolutional layers from (3×3) to (7×7) and then (15×15) without downsampling [12]. However, the convolutional layer of the INet architecture (3×3) is partially used in this study. Fig. 1 shows the proposed brain stroke diagnosis CNN scheme by combination of the C-Net and INet architectures.

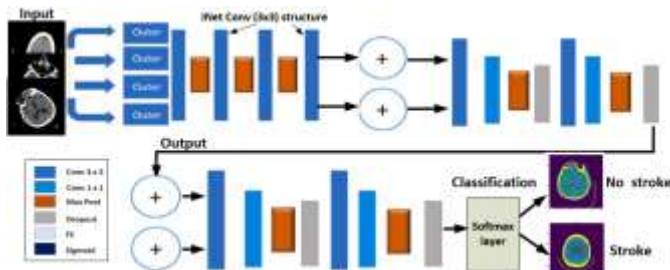


Fig. 1. The proposed hybrid CNN scheme for brain stroke diagnosis

On the C-Net side of the proposed model, various layers and parameters are designed to achieve various important goals, such as brain CT images classification and segmentation. C-Net is a CNN architecture consisting of Outer, Middle, and Inner networks. Using the same deep model in Outer networks provides a more stable and reliable way of feature extraction. Also, using the same (3×3) filter size in convolution layers of INet provides a better way of feature extraction compared to different operations with different filter sizes. INet (3×3) Conv layer structure of the proposed method is represented in Fig. (2), and explained later. Because deep networks operate in parallel, features are extracted by different networks at different times rather than directly connecting to fully connected (FC) layers, and as a result, the shortcomings of one network are compensated for the other network. The proposed model has few parameters with an image size of 256×256 pixels. In the model of each of the Outer networks, first, brain images enter the input layer in all Outer networks simultaneously. After that, it is processed through several convolution layers that do the convolution task represented as (1).

$$(X * K)(i, j) = \sum_m \sum_n \sum_c X(m, n, c) K(m + i - 1, j + n - 1, c) \quad (1)$$

where X defines a three-dimensional brain image that is being convolved by three-dimensional kernel K , sliding over all spatial positions. The first block has a maximum pooling layer. The block here consists of several convolutional layers followed by a pooling layer. The number of filters in the first block is 64 with (3×3) filter size and the same filling, the maximum pooling filter size is (2×2) , and it is repeated in 2 steps for three additional blocks with the same structure and the same order. The number of filters is multiplied by 2 excluding the last block. The maximum pooling layer for the last block has been reduced to prevent further reduction of the final output [15]. Rectified Linear Unite (ReLU) activation function is utilized in the convolution layers as defined in (2).

$$g_{m,n,c} = \max(0, w_c^T x_{m,n}) \quad (2)$$

where (m, n) denotes the parameters for the feature map, c denotes the channel index, w denotes the filter, and $x_{m,n}$ indicates the input at location (m, n) . The returning features of the output are then concatenated, as represented by \oplus operator in Fig. 1. This f operation is applied two by two on all of the output of the Outer networks as defined in (3).

$$f(y, w) = \left((y_{m,n,c_i}) \oplus (w_{m,n,c_j}) \right) = X_{y_{m,n,c_i+c_j}} \quad (3)$$

where y and w denote feature maps of different networks, (c_i, c_j) denotes the number of channels in each output. Input of Middle networks are features extracted from Outer networks. Middle networks consist of four overlapping convolution layers, each with a (3×3) filter size, the same padding, and 256 filters. A (1×1) convolution is placed on top of previous convolutions to reduce the complexity of the model and feature maps. The feature maps obtained from the Middle networks are concatenated as in Eq. (3). This concatenation acts as the input for the Inner network. In this way, it is ensured that each network has the maximum pooling layer when generating efficient feature descriptors. Dropping, which randomly closes some components of the layers, is a normalization method. It also has the feature of preventing the network from over-learning. This process has been applied to each block of the Middle networks. Finally, the Inner network takes as input the features came back by the Middle networks. The Inner network consists of two convolution layers with filter size (3×3) and step 1, a block with the same padding and 256 filters. Also, the proposed model has a (1×1) convolution layer with the same structures, a size (2×2) , and a 2-step maximum pooling layer. ReLU is utilized as the activation function in the Inner network. The inner network's maximum pooling layer is converted into a vector and coupled to an FC layer. After that, it is connected to another FC layer with an equal number of units. Both FC layers have been subjected to a release treatment. Finally, the sigmoid activation function has been used as shown in (4) and (5), respectively [15].

$$z = w^T x + b \quad (4)$$

$$\hat{y} = \text{Sig}(z) = \frac{e^z}{e^z + 1} \quad (5)$$

where z denotes the dot product of filter w with a part of the image with same filter size, and b denotes the bias. The loss function is a cross-entropy function given as (6).

$$L(\hat{y}, y) = -(\sum_{i=1}^N y_i \log \hat{y}_i + (1 - y_i) \log(1 - \hat{y}_i)) \quad (6)$$

where y_i denotes the i th label y of N classes, and \hat{y}_i denotes the i th element of output \hat{y} . A total time complexity of the convolutional layers is computed as in (7).

$$C(\sum_{i=1}^l n_{i-1} \cdot f_i^2 \cdot c_i \cdot m_i^2) \quad (7)$$

where n_{i-1} and c_i denote the number of the input channels and filter channels in the i th layer, respectively, f_i denotes the filter size, and m_i denotes the output feature map size. The time may be decreased by the factor $\frac{1}{4}$ by adding a pooling layer with the same stride with (2×2) in each layer.

In addition to the C-Net architecture, the proposed hybrid model also integrates the superior features of the INet architecture, such as residual shortcuts and convolution index features. In this model, it combines the output feature maps of all previous convolution layers to extract features against kernels of different sizes [12]. Besides, the large kernel deep network is suitable for biomedical image classification and segmentation [18]. As can be seen in Fig. 1, a softmax layer has been used in the brain image classification process. The softmax layer ensures that the deep network output is a class rather than a numerical prediction [5]. This softmax is used in accordance with the class concept because it is desired to detect a brain CT image as non-stroke or stroke. While representing a non-stroke or non-stroke class here, it is expected that there will be a probability value for each class in the output of the proposed model. That is, the input values given to softmax are a kind of non-normalized version of the prediction values. Therefore, the more classes there are, the more output is obtained. In this study, 2 classes are represented as output. The softmax probability calculation (\bar{p}_w) is calculated as (8).

$$\bar{p}_w = \frac{e^{u_w}}{\sum_k e^{u_k}} \quad (8)$$

For the normalization process, the data whose probability is to be calculated must be divided by the sum of all data. Thanks to this operation, the probability sums \bar{p}_w that is the probability sum of all classes become 1. In order for the sum of u_w and u_k in the formula to comply with the probability axiom, both rules must be satisfied. There are two options for providing the first rule: taking it in absolute value or expressing it as exponential.

Fig. 2 shows the designed residual shortcuts and convolutional index of INet. The right-hand side of Fig. 2 shows the residual shortcuts. It denotes the underlying second-last Conv mapping a Conv-layer as $G_i(x_i)$ and $H_i[G_i(x_i)]$, respectively. The stacked Convs fit another mapping: $D_i(x_i) = G_i(x_i) - x_{i-1}$ and $F_i[G_i(x_i)] = H_i[G_i(x_i)] - x_i$, respectively. Once $D_i(x_i)$ covers (i.e., $G_i(x_i) = x_{i-1}$), INet method optimizes $F_i(x_{i-1}) = H_i(x_{i-1}) - x_i$ instead of skipping the last Conv layer. Also, the method performs identity mapping as the basic residual shortcut (i.e., $H_i[G_i(x_i)] = x_i$). The left-hand side of Fig. 2 shows the convolutional index $G_{i-1}(x_{i-1})$. This index lets INet to skip the Inner Convs between the second Conv-layer and the last third Conv-layer. It is considered the feature maps concatenation as giving equal importance to all preceding Conv-layers in INet [12], [22]. The convolutional index is a larger weight on the output feature maps of the

previous Conv-layer that includes the highest level semantics. Heavily, Conv-index enables INet removes the feature maps concatenation. In the proposed CNN, it is considered a Conv-layer to be defined as (9) and (10).

$$G_i(x_i) = D_i(x_i) + x_{i-1} + G_{i-1}(x_{i-1}) \quad (9)$$

$$H_i(x_i) = F_i[G_i(x_i)] + x_i \quad (10)$$

As shown in Fig. 1, the output of the proposed deep learning network architecture consists of two nodes, no-stroke and stroke. As mentioned before, a softmax layer has been used as the classification method, and 2 classes have been defined. So, it is determined whether there is a stroke or not from the brain CT images.

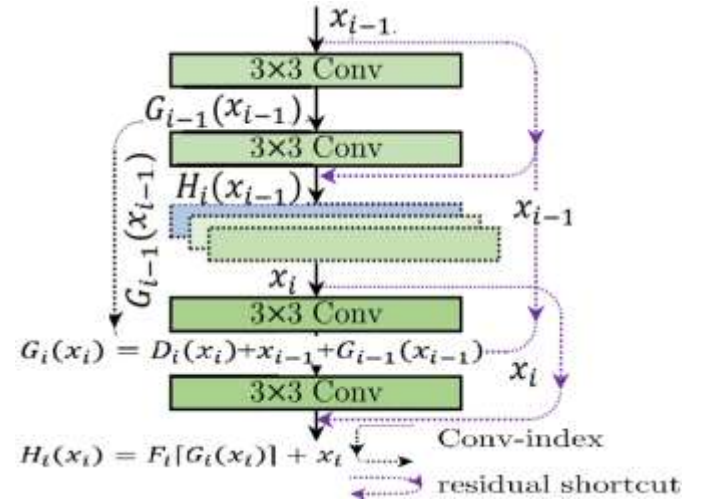


Fig. 2. INet structure in the proposed method. The designed (3×3) conv layers with residual shortcuts and convolutional index of INet

III. EXPERIMENTAL ANALYSIS AND RESULTS

A. The Data Set Used in This Study

The Ministry of Health of the Republic of Turkey donated a data collection that included processed 256×256 pixel DICOM brain CT images. The data set contains 6650 CT brain scans, 4427 of which were stroke-free and 2223 of which were. To add more data to the brain imaging, data augmentation techniques have been used. It was given horizontal flipping and 20% rotation interval approaches, which stopped it from learning from unimportant characteristics and improved its performance as a whole [21]. To enhance the classification and segmentation performance even more, it has been decided to increase the amount of photos. The number of photographs with stroke has been doubled to 4446 because there are significantly fewer images with stroke than without. These strategies for data augmentation were used to add 80% of the data required for training and testing the classification model to the training set, and the remaining 20% was used for testing. Table 1 displays the number of brain CT scans utilized for training and testing in the dataset. In total, there are 7099 images in the training set of the classification model, of which 3542 are CT scans devoid of evidence of a stroke and 3557 are CT images containing such signs. Several CT scans of the brain are shown in Fig. 3. The photos in Fig. 3(a) are of some non-strokes. Images of various

strokes caused by ischemia or hemorrhage are shown in Fig. 3(b).

TABLE I
THE NUMBERS OF BRAIN CT IMAGES FOR TRAINING AND TEST IN THE DATASET

Type of operation	No stroke	Stroke
For Training	3542	3557
For Test	885	889

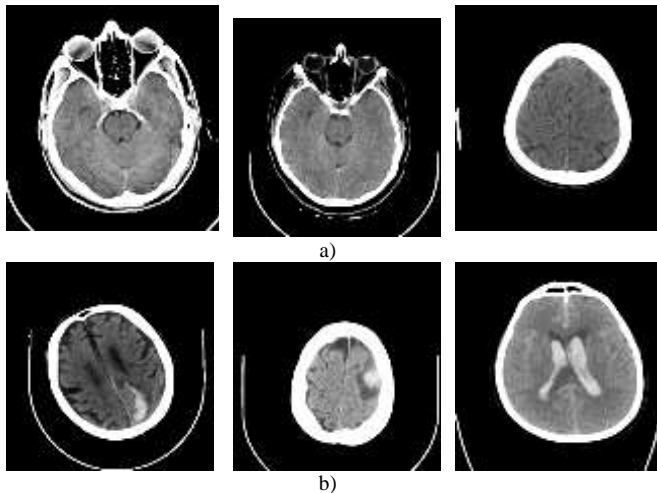


Fig. 3. Some CT brain images of (a) no stroke (b) brain stroke in the dataset

B. Experimental Setup

The proposed method and other models have been implemented on Windows 10 operating system running Intel Core™ i7-8700 processor and 16 GB RAM, Nvidia Geforce 4GB Graphics Card device using Python 3.8 programming for the experiments. Keras [23] and Tensorflow [24] libraries are utilized for training the proposed network. The deep learning framework is Pytorch 1.7.1 based on CUDA Toolkit10.0. In the experiments, image preprocessing methods have been applied to achieve better image quality in classification and segmentation. Table 2 presents several parameters used in this study.

TABLE II
SEVERAL PARAMETERS USED IN THIS STUDY

Parameters	Definition
Convolution layer kernel size	(3 x 3) kernel size used
Output nodes	2 classes classification (no stroke or stroke)
Learning rate	0.001
Optimization method	Adam
Batch size	16
Number of epochs	100
Dropout	0.5

To evaluate the proposed model, precision (*Prc*), true positive rate (*Recall*), false positive rate (*FPR*), *F1-score*, and accuracy (*Acc*) as the evaluation metrics are defined, and calculated in (11), (12), (13), and (15), respectively [21].

$$Prc = \frac{TP}{TP+FP} \quad (11)$$

$$Recall = \frac{TP}{TP+FN} \quad (12)$$

$$FPR = \frac{FP}{FP+TN} \quad (13)$$

$$F1 - score = 2 \cdot \frac{Prc \times Recall}{Prc + Recall} \quad (14)$$

$$Acc = \frac{TP+TN}{TP+TN+FP+FN} \quad (15)$$

$$MCC = \frac{(TP \times TN) - (FP \times FN)}{\sqrt{(TP+FN) \times (TP+FP) \times (FP+TN) \times (TN+FN)}} \quad (16)$$

where *TP*, *TN*, *FP*, and *FN* denote the true positive, true negative, false positive, and false negative, respectively. Also, Matthews Correlation Coefficient (MCC) is evaluated as given in Eq. (16). The MCC generates a high score when the network model has gained superior performance on all the groups of confusion matrix including *TN*, *TP*, *FN*, and *FP*, as more unbiased and reliable than the accuracy.

C. The Results of Brain Stroke Classification and Segmentation

This section evaluates the brain CT images classification and segmentation results. The results of classification as no stroke or stroke in an image from brain images are presented, and then if there is a stroke in an image, the region of the image with the stroke is segmented.

Fig. 4 shows the confusion matrices for ResNet50v2 and UNet, Fig. 5 shows the confusion matrices for DeepLabV3 and ResUNet, Fig. 6 shows the confusion matrices for DenseINet and ResDenseUNet. The confusion matrices for C-Net and the proposed model are shown in Fig. 7 as experimental analysis findings for the categorization of stroke in brain CT images. The true class and the expected class are the two classes in which the confusion matrices are indicated. With this classification, it has been found how many of the brain images in the form of non-stroke or stroke have been estimated correctly. It is clearly seen that the least number of mistakes in stroke predictions are performed by using the proposed method. Table 3 presents the brain stroke classification performance results calculated from the confusion matrices. From the results of method performances, it is clearly deduced that the proposed method, C-Net, ResDenseUNet, DenseINet, ResUNet, DeepLabV3, UNet, and ResNet50v2 achieved at 99.43%, 99.32%, 99.1%, 99.21%, 99.1%, 98.87%, 98.65%, and 98.42% in precision, 99.66%, 99.43%, 99.43%, 99.32%, 99.1%, 98.76%, 98.53%, and 98.2% in recall, 99.54%, 99.37%, 99.26%, 99.26%, 99.1%, 98.81%, 98.58%, and 98.3% in F1-score, 99.54%, 99.37%, 99.26%, 99.26%, 99.09%, 98.81%, 98.59%, and 98.3% in accuracy, 99.1%, 98.76%, 99.53%, 98.53%, 98.2%, 97.63%, 97.18%, and 96.62% in MCC performances, respectively. Fig. 8 shows the accuracy results of the proposed model. It is understood that the accuracy rate of the proposed model is 99.54% after 100 epochs are completed. Fig. 9 shows the loss results of the proposed model. It is clearly understood that the loss rate of the proposed model is very low, almost zero. According to all these classification results, the best performances are obtained with the proposed model, and the proposed model outperformed other methods in terms of various benchmarks.

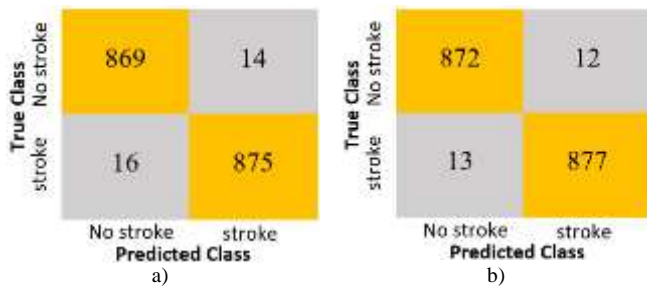


Fig. 4. Confusion matrix of the brain stroke classification results using a) ResNet50v2, b) UNet



Fig. 6. Confusion matrix of the brain stroke classification results using a) DenseINet, b) ResDenseUNet.

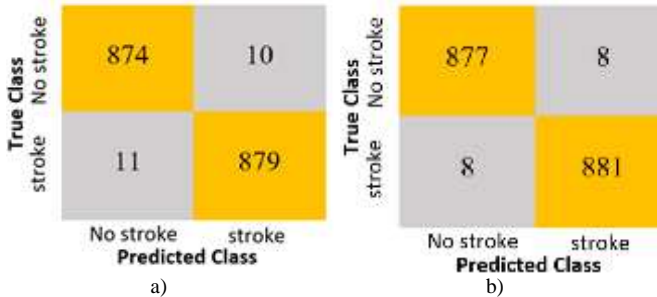


Fig. 5. Confusion matrix of the brain stroke classification results using a) DeepLabV3, b) ResUNet.

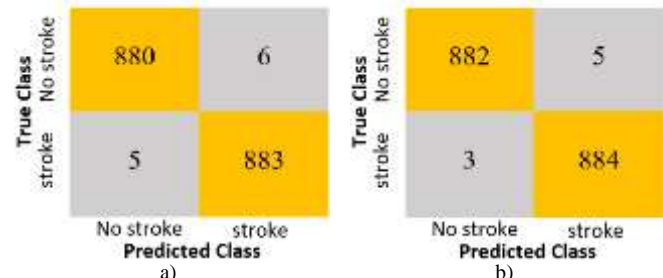


Fig. 7. Confusion matrix of the brain stroke classification results using a) C-Net b) Proposed Model

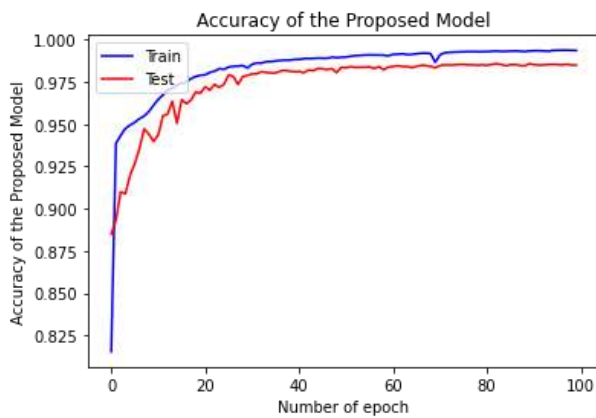


Fig. 8. Accuracy of the proposed model

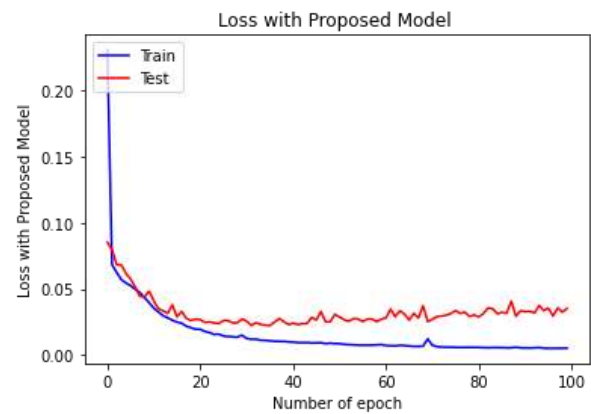


Fig. 9. Loss of the proposed model

TABLE III
PERFORMANCE RESULTS OF THE BRAIN STROKE CLASSIFICATION

Authors	Method	Prc	Recall	FPR	F1-score	Acc	MCC
Rahimzadeh and Attar (2020)	ResNet50v2	0.9842	0.9820	0.0158	0.9830	0.9830	0.9662
Ranneberger <i>et al.</i> (2015)	UNet	0.9865	0.9853	0.0135	0.9858	0.9859	0.9718
Chen <i>et al.</i> (2017)	DeepLabV3	0.9887	0.9876	0.0113	0.9881	0.9881	0.9763
Zhan <i>et al.</i> (2018)	ResUNet	0.9910	0.9910	0.0090	0.9910	0.9909	0.9820
Weng and Zhu (2021)	DenseINet	0.9921	0.9932	0.0079	0.9926	0.9926	0.9853
Khened <i>et al.</i> (2019)	ResDenseUNet	0.9910	0.9943	0.0090	0.9926	0.9926	0.9853
Barzekar and Yu (2022)	C-Net	0.9932	0.9943	0.0067	0.9937	0.9937	0.9876
	Proposed Model	0.9943	0.9966	0.0056	0.9954	0.9954	0.9910

The segmentation is made as follows. Images are divided a visual input into segments to make image analysis easier. Segments consist of one or more sets of pixels. While brain stroke segmentation breaks down pixels into larger components, there is also no need to view each pixel as a unit. It is the process of dividing an image into endurable segments or tiles. The stroke segmentation process begins with the identification of small regions on an image that should not be split. These areas are called strokes, and the position of these seeds defines the tiles. Fig. 10 illustrates the segmentation

estimation results of brain images. Fig. 10(a) shows the original brain CT image. If there is a brain stroke from this overlay image, the stroke region is detected and segmented. The presence of overlay images (ground truth) in Fig. 10(b) indicates that radiologists have confirmed stroke images. The stroke area obtained from the stroke brain images approved by the radiologists is scanned in red. In Fig.10(c), the proposed model result is obtained, and the brain stroke regions scanned in green are given. As can be seen from these results, the estimation of stroke from brain CT images and the detection of

the borders of the stroke region are quite successful. In addition, results very similar to the stroke areas determined by radiologists are obtained that are available in the dataset. Fig. 11 shows some estimations and segmentations of brain stroke. Here, some brain images with size of 256 x 256 are masked to make them dynamic with contrast, and strokes from masked images have been more easily detected.

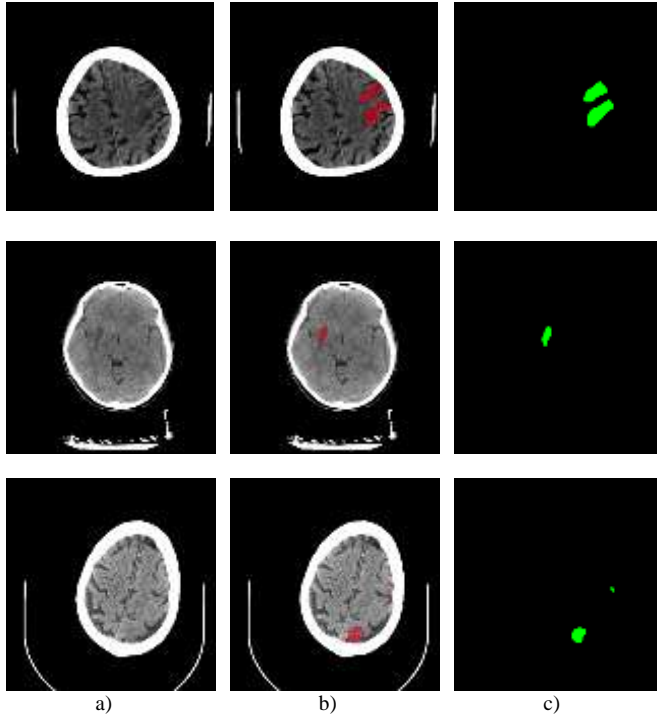


Fig. 10. Brain stroke estimations and segmentations a) original images b) stroke images confirmed by radiologists (overlay images) c) estimated and segmented images

Note that ten experts annotated ground truth maps for the evaluation of segmentation performance. The results of the segmentation are approved by 10 highly experienced radiologists. The Intersection over Union (IoU) and Dice Coefficient (DC) values are measured to prove the accuracy of the segmentation process.

Here, we want to evaluate how well spatial segmentation zones are predicted from photos of brain strokes. The IoU and DC computations are shown in Fig. 12. The IoU value is determined as a percentage of the number of pixels that are different from 0 at the intersection of the M_p and M_d pictures, as well as the intersection of the M_p and M_e images, as in (17).

$$IoU = \frac{S(Rectangle1 \cap Rectangle2)}{S(Rectangle1 \cup Rectangle2)} \quad (17)$$

where M_d signifies the image acquired by the dilation operation using the 3x3 convolution matrix of the mask image, M_e means the image obtained by the erosion operation using the 3x3 convolution matrix of the mask image, and M_p defines the picture produced by the segmentation model. Each image's IoU value is determined separately, and when evaluating the models, the average of these values was taken into consideration. Rectangles 1 and 2 are presumptively

represented by $[x1, y1, x2, y2]$ and $[x3, y3, x4, y4]$, respectively. The stroke segmentation zones are calculated using this convention.

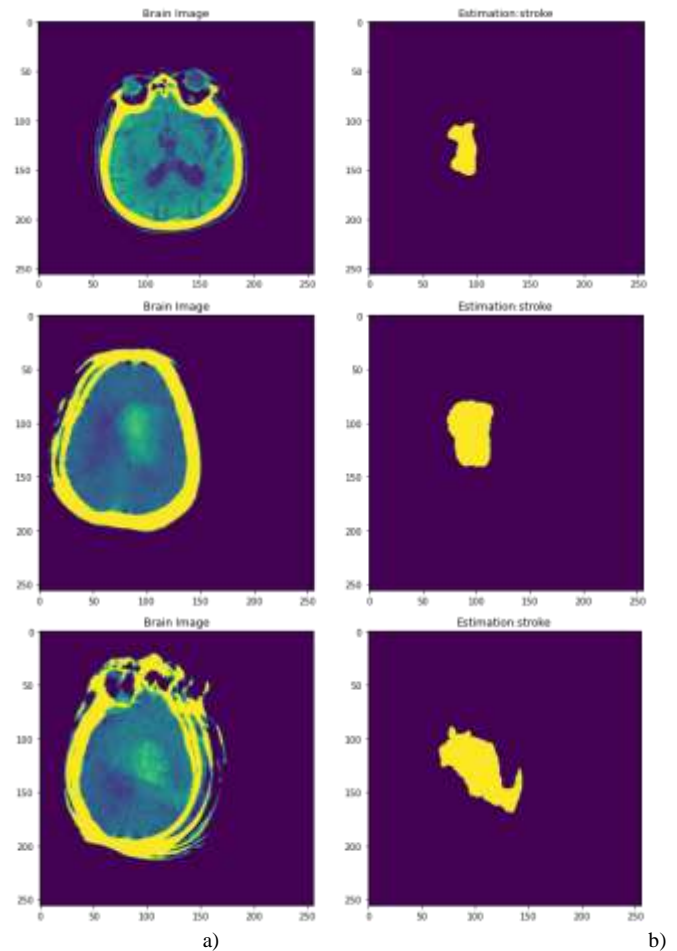


Fig. 11. Some estimations and segmentations of brain stroke a) masked images b) estimated and segmented of stroke

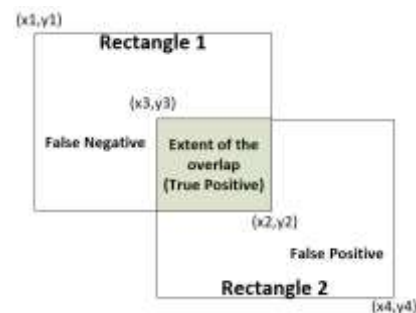


Fig. 12. Representation of the Intersection over Union (IoU) and Dice Coefficient (DC)

Accordingly, the Dice Coefficient (DC), which is also known as the Sørensen–Dice Coefficient, is defined as two times the area of the extent of the overlap, divided by the sum of the areas of Rectangle 1 and Rectangle 2 as given in (18):

$$DC = \frac{2x S(Rectangle1 \cap Rectangle2)}{S(Rectangle1) + S(Rectangle2)} \quad (18)$$

The proposed model produces a higher IoU and DC accuracy rates and a lower loss rate in the experiments.

The average IoU and DC performance results are shown in Table 4. The proposed method, C-Net, ResDenseUNet, DenseINet, ResUNet, DeepLabV3, UNet, and ResNet50v2 achieved at 97.97%, 97.52%, 96.73%, 95.83%, 95.16%,

94.37%, 93.47%, and 93% in IoU, 98.97%, 98.74%, 98.34%, 97.87%, 97.52%, 97.1%, 96.62%, and 96.38% in DC, respectively.

TABLE IV
PERFORMANCE RESULTS OF THE BRAIN STROKE SEGMENTATION

Authors	Method Name	Intersection-over-Union (IoU)	Dice Coefficient (DC)
Rahimzadeh and Attar (2020)	ResNet50v2	0.93	0.9638
Ranneberger <i>et al.</i> (2015)	UNet	0.9347	0.9662
Chen <i>et al.</i> (2017)	DeepLabV3	0.9437	0.971
Zhan <i>et al.</i> (2018)	ResUNet	0.9516	0.9752
Weng and Zhu (2021)	DenseINet	0.9583	0.9787
Khened <i>et al.</i> (2019)	ResDenseUNet	0.9673	0.9834
Barzekar and Yu (2022)	C-Net	0.9752	0.9874
	Proposed Model	0.9797	0.9897

IV. CONCLUSION

In this paper, a brain stroke classification and segmentation method is proposed using C-Net and INet based CNN methods. Brain CT images are classified as no stroke or stroke using the proposed hybrid CNN model. Moreover, the proposed model finds the location and area of the brain stroke region with its boundaries by the segmentation method. To test the proposed model, several performance analyzes are performed with existing CNN methods such as ResNet50v2, UNet, DeepLabV3, ResUNet, DenseINet, ResDenseUNet, and C-Net using Python programming. From the performance results, it is concluded that the proposed model is better than other methods such as precision, recall, FPR, F1-score, accuracy, and MCC in classification and segmentation of the brain CT images. It is considered that the applying the proposed model for brain stroke diagnosis may be so useful for healthcare professionals in most medical applications. In future studies, it is planned to apply the proposed CNN model to the detection and classification of multiple diseases occurring in the abdomen or cardiovascular system.

V. ACKNOWLEDGMENT

The General Directorate of Health Information Systems of the Ministry of Health of the Republic of Turkey is thanked by the author for supplying the information for this study. According to Article 28 of the Law on Protection of Personal Data No. 6698 of the Republic of Turkey and Article 16 of the Regulation on Personal Health Data No. 30808, which was passed in accordance with the applicable law, this scientific investigation was conducted.

REFERENCES

- [1] S. Park, et al. "Annotated normal CT data of the abdomen for deep learning: Challenges and strategies for implementation", *Diagnostic and Interventional Imaging*, Vol. 101, No. 1, 2020, pp.35-44.
- [2] H. Huang, et al. "UNet 3+: A Full-Scale Connected UNet for Medical Image Segmentation", *Electrical Engineering and Systems Science, Image and Video Processing*, 2020, <https://doi.org/10.48550/arXiv.2004.08790>.
- [3] N. Dey, V. Rajinikanth, "Automated detection of ischemic stroke with brain MRI using machine learning and deep learning features", *Magnetic*

- Resonance Imaging, Recording, Reconstruction and Assessment Primers in Biomedical Imaging Devices and Systems, 2022, pp.147-174.
- [4] A. Gautam, B. Raman, "Towards effective classification of brain hemorrhagic and ischemic stroke using CNN", *Biomedical Signal Processing and Control*, Vol. 63, Article 102178, 2021.
- [5] B.R. Gaidhani, R. Rajamenakshi, S. Sonavane, "Brain Stroke Detection Using Convolutional Neural Network and Deep Learning Models", 2019 2nd International Conference on Intelligent Communication and Computational Techniques (ICCT), Jaipur, Sep 28-29, 2019, pp. 242-249.
- [6] C.M. Lo, P.H. Hung, D.T. Lin, "Rapid Assessment of Acute Ischemic Stroke by Computed Tomography Using Deep Convolutional Neural Networks", *Journal of Digital Imaging*, Vol. 34, 2021, pp. 637-646.
- [7] N. Tomitaa, S. Jiangb, M.E. Maeder, S. Hassanpour, "Automatic post-stroke lesion segmentation on MR images using 3D residual convolutional neural network", *NeuroImage: Clinical*, Vol. 27, 2020,102276.
- [8] V. Badrinarayanan, A. Kendall, R. Cipolla, "Segnet: A deep convolutional encoder-decoder architecture for image segmentation", *IEEE transactions on pattern analysis and machine intelligence*, Vol. 39, No. 12, 2017, pp.2481-2495.
- [9] O. Ronneberger, P. Fischer, T. Brox, "U-Net: Convolutional Networks for Biomedical Image Segmentation", *Medical Image Computing and Computer-Assisted Intervention – MICCAI 2015*, 2015, pp.234-241.
- [10] L. Liu, S. Chen, F. Zhang, F.X. Wu, Y. Pan, J. Wang, "Deep convolutional neural network for automatically segmenting acute ischemic stroke lesion in multi-modality MRI", *Neural Computing and Applications*, Vol. 32, 2020, pp.6545-6558.
- [11] Z. Zhang, Q. Liu, Y. Wang, "Road extraction by deep residual UNet," *IEEE Geosci. Remote Sens. Lett.*, Vol. 15, No. 5, pp. 749-753, May 2018.
- [12] W. Weng, X. Zhu, "INet: Convolutional Networks for Biomedical Image Segmentation", *IEEE Access*, Vol. 9, 2021, pp.16591-16603.
- [13] M. Khened, V. A. Kollerathu, G. Krishnamurthi, "Fully convolutional multi-scale residual DenseNets for cardiac segmentation and automated cardiac diagnosis using ensemble of classifiers", *Med. Image Anal.*, Vol. 51, pp. 21-45, Jan. 2019.
- [14] G.S. Saragih, et al. "Ischemic Stroke Classification using Random Forests Based on Feature Extraction of Convolutional Neural Networks", *International Journal on Advanced Science Engineering Information Technology*, Vol. 10, No. 5, 2020, pp.2177-2182.
- [15] H Barzekar, Z. Yu, "C-Net: A reliable convolutional neural network for biomedical image classification", *Expert Systems With Applications*, Vol. 187, 2022, 116003.
- [16] I. Oksuz, "Brain MRI artefact detection and correction using convolutional neural networks", *Computer Methods and Programs in Biomedicine*, Vol. 199, 2021, 105909.

- [17] A. Deshpande et al. “ Automatic segmentation, feature extraction and comparison of healthy and stroke cerebral vasculature”, *NeuroImage: Clinical*, Vol. 30, 2021, 102573.
- [18] Y. Zhou, W. Huang, P. Dong, Y. Xi, S. Wang, “D-UNet: A Dimension-Fusion U Shape Network for Chronic Stroke Lesion Segmentation”, *IEEE/ACM Transactions on Computational Biology and Bioinformatics*, Vol. 18, No. 3, 2021, pp.940-950.
- [19] M. Rahimzadeh, A. Attar, “A modified deep convolutional neural network for detecting COVID-19 and pneumonia from chest X-ray images based on the concatenation of Xception and ResNet50V2”, *Informatics in Medicine Unlocked*, Vol. 19, 2020, 100360.
- [20] L.-C. Chen, G. Papandreou, F. Schroff, H. Adam, “Rethinking atrous convolution for semantic image segmentation”, arXiv:1706.05587. [Online]. 2017, Available: <http://arxiv.org/abs/1706.05587>.
- [21] S. Yalçın, H. Vural, “Brain stroke classification and segmentation using encoder-decoder based deep convolutional neural networks”, *Computers in Biology and Medicine*, Vol. 149, 2022, 105941.
- [22] K.S. A. Kumara, A.Y. Prasad, J. Metan, “A hybrid deep CNN-Cov-19-Res-Net Transfer learning architype for an enhanced Brain tumor Detection and Classification scheme in medical image processing”, *Biomedical Signal Processing and Control*, Vol. 76, 2022, 103631.
- [23] F. Chollet, et al. Keras. <https://github.com/fchollet/keras>, 2015.
- [24] M. Abadi, et al. “Tensorflow: A system for large-scale machine learning”, In 12th {USENIX} Symposium on Operating Systems Design and Implementation ({OSDI} 16), 2016, pp. 265–283.

BIOGRAPHIES



Sercan YALÇIN received his BSc in Computer Engineering from Firat University, Turkey in 2013. He received his MSc and PhD in Computer Engineering, Firat University, Turkey in 2016 and 2021, respectively. He currently works at Adıyaman University. His research interests include wireless networks, data science, and artificial intelligence.